

Optimizing the external optical cavity parameters for performance improvement of a fiber grating Fabry–Perot laser

Hisham Kadhum Hisham · Ahmad Fauzi Abas ·
Ghafour Amouzad Mahdiraji · Mohd Adzir Mahdi ·
Faisal Rafiq Mahamd Adikan

Received: 10 June 2014 / Accepted: 9 January 2015 / Published online: 4 March 2015
© The Optical Society of Japan 2015

Abstract The effects of the external optical cavity parameters (external optical cavity length (L_{ext}), amplitude coupling (C_o) and anti-reflection coating (ARC) reflectivity coefficients) on the noise and modulation spectra of a fiber grating Fabry–Perot laser are numerically analyzed for designing a laser that operates in strong feedback regime (Regime V). Fiber Bragg grating (FBG) is used as a wavelength selective element to control the properties of the laser output by controlling the external optical feedback (OFB) level. The study is performed by modifying a set of rate equations that are solved by considering the effects of external OFB and ambient temperature (T) variations. We proposed a model to calculate the temperature dependence (TD) of laser characteristics according to the TD of laser parameters. An accurate analytical expression for the TD of threshold carrier density ($N_{\text{th,fe}}$) has been derived. The TD of $N_{\text{th,fe}}$ was calculated according to the TD of laser cavity

parameters instead of using well-known empirical Pankove relationship via the use of characteristics temperature (T_o) and current (I_o). Results show that the optimum external fiber length (L_{ext}) is 3.1 cm. Also, it is shown that ARC with reflectivity value of 1×10^{-2} is sufficient for the laser to operate at low noise, good modulation response, and low fabrication complexity.

Keywords External cavity semiconductor lasers · External optical feedback · Fiber Bragg grating

1 Introduction

Among all types of lasers, semiconductor laser diodes (SLDs) are predominately used for optical communication systems. They have been widely used in wavelength-division-multiplexing (WDM) systems due to small size, low power consumption, and their ability to perform direct modulation at moderate bit rates [1–8]. On the other hand, the incessant increase in the users of optical communication systems demands very high speed data transmission [9–11]. Having the ability of high speed modulation, SLDs become an excellent option for WDM systems. However, a major obstacle preventing closer WDM channel spacing is the drift of emission wavelength with temperature variation [12–21]. Therefore, with the development of dense WDM (DWDM) systems, lasers with narrow linewidth, high side-mode suppressed ratio (SMSR), low chirp, low cost, fast response, and stable dynamic single-mode operation are indispensable [1–12].

Thus far, in current WDM systems, distributed feedback (DFB) laser diodes have been commonly used as the light sources. However, their lasing wavelengths are affected with temperature (e.g., 100 pm/K) and injection current

H. K. Hisham (✉)
Department of Electrical Engineering, Faculty of Engineering,
Basra University, Basra, Iraq
e-mail: husham_kadhum@yahoo.com

A. F. Abas · M. A. Mahdi
Department of Computer and Communication Systems
Engineering, Faculty of Engineering, Wireless and Photonic
Networks Research Center, Universiti Putra Malaysia, UPM,
43400 Serdang, Selangor, Malaysia

A. F. Abas
Department of Electrical Engineering, College of Engineering,
King Saud University, P.O. Box 800, Riyadh 11421,
Kingdom of Saudi Arabia

G. Amouzad Mahdiraji · F. R. Mahamd Adikan
Integrated Lightwave Research Group, Department of Electrical
Engineering, Faculty of Engineering, University of Malaya,
50603 Kuala Lumpur, Malaysia

(e.g., 10 pm/mA) [9, 10, 13, 16, 21]. Therefore, accurate temperature controller and wavelength-locking devices should be used to avoid optical cross-talks between the adjacent channels originated from wavelength shift, especially in DWDM systems. This ultimately leads to a high-cost light source. The additional cost can be avoided by capitalizing on the high stability of silica with temperature (10 pm/K [4–6, 9, 11–24]) in external cavity configurations using fiber Bragg grating (FBG).

In recent years, fiber grating Fabry–Perot (FGFP) laser is proposed as an alternative light source for WDM systems, which can generate output with high wavelength stability [23–30]. This is because the emission wavelength of FGFP laser depends only on the Bragg wavelength of fiber grating (FG), thus, independent of chip temperature and injection current. Moreover, the lasing wavelength tuning can be performed accurately because the grating period of FBG can be controlled with high accuracy of ± 0.1 nm [4–6, 9, 11–30]. Therefore, precise adjustment of the Bragg wavelength in FG is easier in comparison to the emission wavelength of DFB lasers. The main advantages of a SLD with external FG resonator are high-speed direct modulation with low chirping effect, enhanced wavelength stability, and relatively cost effective [6, 9, 13, 16, 21, 23–30].

On the other hand, transmission experiments have shown that a DWDM system using a directly modulated FGFP laser has an order of magnitude better tolerance to transmitter temperature variations as compared to directly or externally modulated DFB lasers [6, 16, 17, 22, 32, 35, 36]. As a result, in comparison to the DFB laser, FGFP lasers have higher lasing wavelength stabilities with temperature and current, and therefore, can be used without high precision temperature controller [6, 16, 17, 22, 32, 35, 36].

In addition, the dynamic behavior of the external cavity semiconductor laser (ECSL) under the effect of external OFB can be divided into five regimes based on the feedback intensity level [37]. In regime I, the feedback is quite small; the laser linewidth is increased or decreased depending on the phase of the delayed light coupled into the laser diode (LD). With the increase of the feedback the LD will operate in regime II, where mode hopping among several external cavity modes can be observed. Further increase in the feedback level will bring the LD into regime III and IV, where the linewidth of the LD is drastically broadened and the chaos can be seen in these regimes. In the new regime V, where there is very high feedback level, the internal and external cavities behave like a single cavity and the laser oscillates in a single mode. The linewidth of the laser in this regime is very narrow [38]. Therefore, regime V laser source is very important for satisfying the DWDM systems requirements, and optimizing laser external OFB level is very essential.

An important design parameter of the ECSL based on fiber grating is the external optical cavity parameters (external optical cavity length (L_{ext}), amplitude coupling (C_o), and the value of the ARC reflectivity coefficients), which should be optimized to emit laser radiation with minimum intensity noise and stable spectrum. Ahmed and Tucker [39], have shown that by optimizing the external cavity length L_{ext} , the resonance peak spectral splitting (RPSS) from the modulation response spectra can be suppressed. Also, they have found the high coupling between active and passive cavities lead to a lack of the RPSS appearance. On the other hand, the reflectivity value of the ARC front facet (R_o) of Fabry–Perot (FP) laser is one of the important parameters in determining the performance of the ECSL. Furthermore, it has been found that the bistability, multi-stability, mode hopping-induced instability, and continuous frequency tuning range are dependent on the reflectivity value of the ARC of laser diode [40]. In addition, it has been shown that by reducing the reflectivity value of the ARC as low as possible, the ECSL performance can be improved [41].

Although many experimental and theoretical studies have reported on the ECSL characteristics [4–6, 9, 11, 13, 16, 17, 21, 22, 29–43], the effects of the external optical cavity parameters on the ECSL-based FG performance are yet to be investigated. In this paper, we conducted a numerical analysis on the effect of the external optical cavity parameters [external optical cavity length (L_{ext}), amplitude coupling (C_o) and ARC reflectivity coefficients] on the FGFP laser performance. The TD of I_{th} has been empirically described by the well-known exponential Pankove relationship using two parameters T_o and I_o known as the characteristics of both temperature and current [34, 44]. In this study, the TD of I_{th} has been investigated according to TD of laser cavity parameters. The obtained results can provide important data for practical fabrication of the FGFP laser.

The paper is structured as follows: the Fiber Grating Fabry–Perot (FGFP) laser model is given in the next section. Section 3 presents the Rate equations for FGFP laser. In Sect. 4, we demonstrate the FGFP Laser Performance. The simulation results are discussed in Sect. 5 followed by the conclusions.

2 Fiber grating Fabry–Perot laser model

The FGFP model consists of three main sections as shown in Fig. 1a. The first section is the Fabry–Perot laser diode (FP-LD) of length L_d . It is assumed that the reflectivity of the chip front facet (R_o) is very low to suppress FP mode oscillation and to stabilize the external cavity mode, while the rear facet has high reflectivity (R_1). The second section is a fiber of length L_{ext} , and the third is the FBG with

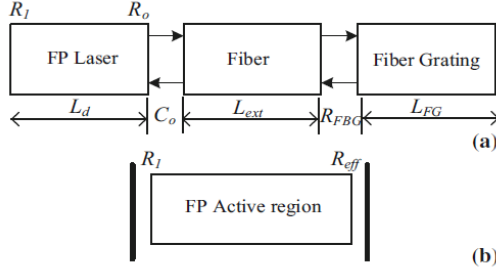


Fig. 1 a Schematic structure of FGFP laser and b simplified configuration 25-30'

reflection coefficient of R_{FBG} . The temperature dependence (TD) on the photons round-trip time inside the internal and the external cavity are $\tau_d(T) = 2n_d(T) L_d/c$ and $\tau_e(-T) = 2L_{ext}n_{ext}(T)/c$, respectively, where c is the velocity of the light in the vacuum, $n_d(T)$ is the TD group refractive index of the FP laser diode, and $n_{ext}(T)$ is the TD fiber refractive index.

This configuration may be conveniently analyzed as a simple two-mirror laser structure (Fig. 1b) by replacing the FP diode laser output facet reflectivity R_o by a complex-valued effective reflection coefficient R_{eff} [24–27, 45–47].

$$R_{eff} = \frac{R_o^2 + R_{OFB}^2 + 2R_o R_{OFB} \cos(\omega\tau_e)}{1 + R_o^2 R_{OFB}^2 + 2R_o R_{OFB} \cos(\omega\tau_e)}, \quad (1)$$

where $\omega\tau_e$ is the phase of the reflected light that travels through the external cavity and ω is the laser angular frequency. In (1), $R_{OFB} = C_o R_{ext}$ is the amount of optical feedback reflection coupled to FP laser diode, where C_o is the amplitude coupling coefficient between the FP laser diode and the grating fiber, and R_{ext} is the power reflectivity of FG defined as [46, 47]

$$R_{ext} = |R_{FBG}|^2 = \begin{cases} \frac{(kL_{FG})^2 \sinh^2(QL_{FG})}{(\Delta\beta L_{FG})^2 \sinh^2(QL_{FG}) + (QL_{FG})^2 \cosh^2(QL_{FG})}, & \text{if } (kL_{FG})^2 > (\Delta\beta L_{FG})^2 \\ \frac{(kL_{FG})^2 \sin^2(\Omega L_{FG})}{(\Delta\beta L_{FG})^2 - (kL_{FG})^2 \cos^2(\Omega L_{FG})}, & \text{if } (kL_{FG})^2 < (\Delta\beta L_{FG})^2 \end{cases} \quad (2)$$

where L_{FG} is the grating length, $\Delta\beta$ is the wavelength detuning, k is the coupling strength, $Q = \sqrt{k^2 - \Delta\beta^2}$, and $\Omega = iQ = \sqrt{\Delta\beta^2 - k^2}$. The phase coefficient for reflection light θ_{ref} is derived from the differential equations in ref. [46] and is given by

$$\theta_{ref} = \begin{cases} \tan^{-1} \left(\frac{Q \cosh(QL_{FG})}{\Delta\beta \sinh(QL_{FG})} \right), & \text{if } (kL_{FG})^2 > (\Delta\beta L_{FG})^2 \\ \tan^{-1} \left(\frac{\Omega \cos(\Omega L_{FG})}{\Delta\beta \sin(\Omega L_{FG})} \right), & \text{if } (kL_{FG})^2 < (\Delta\beta L_{FG})^2 \end{cases} \quad (3)$$

By considering the phase change introduced by the optical filter in Eq. (1), R_{eff} can be rewritten as

$$R_{eff} = \frac{R_o^2 + R_{OFB}^2 + 2R_o R_{OFB} \cos(\omega\tau_e - \theta_{ref})}{1 + R_o^2 R_{OFB}^2 + 2R_o R_{OFB} \cos(\omega\tau_e - \theta_{ref})}. \quad (4)$$

The temperature dependence (TD) of threshold current $I_{th,fe}(T)$ of FGFP laser under the effect of external OFB can be written as [33, 34]

$$I_{th,fe}(T) = qVN_{th,fe}(T) \left(A_{nr} + BN_{th,fe}(T) + C(T)N_{th,fe}^2(T) \right), \quad (5)$$

where q is the electron charge, V is the FP active region volume, A_{nr} describes the non-radiative recombination rate due to traps or surface states, $C(T)$ is the TD Auger process, B is the radiative recombination coefficient, and $N_{th,fe}(T)$ is the TD carrier density at the threshold condition. The $N_{th,fe}(T)$ can be represented by modifying the well-known expression in [33] as

$$N_{th,fe}(T) = N(T) + \frac{1}{\Gamma v_g(T) a(T) \tau_{p,fe}(T)}, \quad (6)$$

where $N(T)$, $a(T)$, and $\tau_{p,fe}(T)$ are the TD parameters that are known as transparency carrier density, gain constant, and photon life time (with the external OFB effect), respectively. Γ denotes the confinement factor, and $v_g(-T) = c/n_d(T)$ is the TD group velocity. The temperature-dependent parameters are assumed to vary with the temperature according to [16]:

$$X(T) = X_o + \frac{\partial X}{\partial T} (T - T_o), \quad (7)$$

where X_o is the initial value found at the reference temperature (T_o), which is considered at the room temperature (25 °C). Since the external OFB only affects on the photon lifetime in Eq. (6), $\tau_{p,fe}(T)$ can be modeled as

$$\tau_{p,fe}(T) = \frac{1}{v_g(T) \alpha_{tot,fe}(T)}, \quad (8)$$

where $\alpha_{\text{tot,fe}}(T)$ is the TD total cavity loss that is defined as [24–30].

$$\alpha_{\text{tot,fe}}(T) = \alpha_{\text{int}}(T) + \frac{1}{2L_d} \ln\left(\frac{1}{R_1 R_{\text{eff}}}\right), \quad (9)$$

where $\alpha_{\text{int}}(T)$ is the TD internal cavity loss, and the term $(1/2L_d) \ln(1/R_1 R_{\text{eff}})$ is the mirror loss. Finally, the $N_{\text{th,fe}}$ can be expressed as

$$N_{\text{th,fe}}(T) = N(T) + \frac{1}{\Gamma a(T)} \left[\alpha_{\text{int}}(T) + \frac{1}{2L_d} \left\{ \ln\left(\frac{1}{R_1}\right) + \ln\left(\frac{1 + 2R_0 R_{\text{OFB}} \cos(\omega\tau_e - \theta_{\text{ref}}) + R_0^2 R_{\text{OFB}}^2}{R_0^2 + 2R_0 R_{\text{OFB}} \cos(\omega\tau_e - \theta_{\text{ref}}) + R_{\text{OFB}}^2}\right) \right\} \right]. \quad (10)$$

Equation (10) gives general expression for threshold carrier density that is used to calculate the net rate of stimulated emission in the active region.

3 Rate equations for FGFP laser

The delayed feedback system is infinity degree of freedom system [48, 49] and in the case of grating optical feedback from the fiber Bragg grating, multiple reflections must be taken into account, especially if the model works in Regime IV [38]; however, by optimizing the laser, we pushed it to work in Regime V. In this case, the rate equations approximation can be used without considering multiple reflections. By considering the effect of temperature and external OFB described in the previous section, the noise characteristics of FGFP laser can be derived from the well-known coupled rate equations [34], after taking into account the effect of external OFB and temperature variation. In this case, different noise sources, $F_i(t)$, including the carrier number, $N(t)$, photon number, $P(t)$, and the optical phase, $\phi(t)$, can be described as

$$\frac{dN(t)}{dt} = \frac{I(t)}{q} - \frac{N(t)}{\tau_{\text{c,fe}}(T)} - g(T) \frac{N(t) - \bar{N}}{1 + \varepsilon(T)P(t)} P(t) + F_N(t) \quad (11a)$$

$$\frac{dP(t)}{dt} = g(T) \frac{N(t) - \bar{N}}{1 + \varepsilon(T)P(t)} P(t) - \frac{P(t)}{\tau_{\text{p,fe}}(T)} + R_{\text{sp,fe}}(T) + F_P(t) \quad (11b)$$

$$\frac{d\phi(t)}{dt} = \frac{1}{2} \alpha_N(T) (N(t) - \bar{N}) + \frac{\arg(R_{\text{ext}})}{\tau_d(T)} + F_\phi(t), \quad (11c)$$

where $I(t)$ is the injection current, $\tau_{\text{c,fe}}(T) = qVN_{\text{th,fe}}(T)/I_{\text{th,fe}}(T)$ is the TD carrier lifetime, $g(T)$ is the TD gain slope constant coefficient, $\varepsilon(T)$ is the TD nonlinear gain compression factor, α is the linewidth enhancement factor, \bar{N} is the time-average carrier number and where $G_N(T) = v_g(T)\Gamma a(T)/V$ is the gain derivative, and $F_N(t)$, $F_P(t)$, and

$F_\phi(t)$ are the Langevin noise sources due to the carriers, photons, and phase, respectively. In Eq. (11), $R_{\text{sp,fe}}(T)$ represents the TD of the modified spontaneous emission rate coupled to the lasing mode, which is defined as [34]

$$R_{\text{sp,fe}}(T) = \beta_{\text{sp}} \eta_{\text{sp,fe}}(T) (A_{\text{nr}} + BN_{\text{th,fe}}(T) + C(T)N_{\text{th,fe}}^2(T))N_{\text{th,fe}}(T), \quad (12)$$

where β_{sp} is the spontaneous emission factor and $\eta_{\text{sp,fe}}(T)$ is the TD spontaneous quantum efficiency.

To obtain the noise characteristics, the fluctuations of the variables in Eq. (11) are assumed to remain small at all times in comparison with the respective steady-state average values (small-signal approximation). Under this assumption, the rate equations can easily be solved numerically in the frequency domain using the Fourier transforms.

The fluctuation of the lasing frequency $\Delta\nu(t)$ is described by the variation of the optical phase as [33, 35]

$$\Delta\nu(t) = \frac{1}{2\pi} \frac{d\phi(t)}{dt}. \quad (13)$$

The random Langevin noise sources in Eq. (11) are assumed to be Gaussian random variables due to the carriers, photons, and phase, respectively. Considering the Markovian assumption, the general relationship between the noise sources can be defined as [34]

$$\langle F_i(t) \rangle = 0 \quad (14)$$

$$\langle F_i(t) \cdot F_j(t') \rangle = 2D_{ij}\delta(t - t'), \quad (15)$$

where angle brackets denote ensemble average, δ is the Dirac's delta function, and D_{ij} are diffusion coefficients associated with the corresponding noise source of i and j , which is defined as [34]

$$D_{\text{SS}} = \frac{R_{\text{sp,OFB}}N(t)S(t)}{\tau_{\text{c,OFB}}} \quad (16)$$

$$D_{\text{NN}} = \frac{N(t)}{\tau_{\text{c,OFB}}} [1 + R_{\text{sp,OFB}}S(t)] \quad (17)$$

$$D_{\phi\phi} = \frac{R_{\text{sp,OFB}}N(t)}{4\tau_{\text{c,OFB}}S(t)} \quad (18)$$

$$D_{\text{SN}} = \frac{-R_{\text{sp,OFB}}N(t)S(t)}{\tau_{\text{c,OFB}}} \quad (19)$$

$$D_{S\phi} = D_{N\phi} = 0 \quad (20)$$

The output power $P_{\text{out}}(t)$ from the front facet of FGFP laser is given by [46]

$$P_{\text{out}}(t) = x \cdot \frac{hc}{\lambda} \cdot \frac{c}{n_d} \cdot \frac{1}{2L_d} \ln\left(\frac{1}{R_1 R_{\text{eff}}}\right) \cdot \text{VP}(t) \quad (21)$$

$$x = \frac{(1 - \sqrt{R_{\text{eff}}})\sqrt{R_1}}{(1 - \sqrt{R_{\text{eff}}})\sqrt{R_1} + (1 - R_1)\sqrt{R_{\text{eff}}}}, \quad (22)$$

where h is the Plank's constant.

4 FGFP laser performance

4.1 Noise characteristics

Numerical simulations of relative intensity noise (RIN) and frequency, or phase noise (FN) of FGFP laser are evaluated from the fluctuations $\delta P(t)$ and $\Delta v(t)$, respectively, that result from time integration of Eq. (11) and using Eqs. (12), (13), (14), (15), (16), (17), (18), (19) and (20). The RIN and FN spectra of FGFP laser are originally defined as the Fourier transform of the auto-correlation functions [24, 27]

$$\text{RIN} = \frac{1}{\langle P_{\text{out}} \rangle^2} \left[\int_0^\infty \delta P_{\text{out}}(t) \delta P_{\text{out}}(t + \tau) e^{j\omega\tau} d\tau \right] \quad (23)$$

$$\text{FN} = \int_0^\infty \Delta v(t) \Delta v(t + \tau) e^{j\omega\tau} d\tau. \quad (24)$$

Then, RIN and FN are calculated over a time period T from the equations

$$\begin{aligned} \text{RIN} &= \frac{1}{\langle P_{\text{out}} \rangle^2} \left\{ \frac{1}{T} \int_0^T \left[\int_0^\infty \delta P_{\text{out}}(t) \delta P_{\text{out}}(t + \tau) e^{j\omega\tau} d\tau \right] dt \right\} \\ &= \frac{1}{\langle P_{\text{out}} \rangle^2} \left\{ \frac{1}{T} \left| \int_0^T \delta P_{\text{out}}(\tau) e^{-j\omega\tau} d\tau \right|^2 \right\} \end{aligned} \quad (25)$$

$$\begin{aligned} \text{FN} &= \frac{1}{T} \left\{ \int_0^T \left[\int_0^\infty \Delta v(t) \Delta v(t + \tau) e^{j\omega\tau} d\tau \right] dt \right\} \\ &= \frac{1}{T} \left| \int_0^T \Delta v(\tau) e^{-j\omega\tau} d\tau \right|^2 \end{aligned} \quad (25)$$

4.2 Modulation characteristics

The FGFP laser modulation characteristics can be developed from the modified well-known expression of single-mode coupled rate equations given in Eq. (11), after removing the Langevin noise sources due to the carriers, photons, and phase, $F_N(t)$, $F_P(t)$, and $F_\phi(t)$, respectively.

For a small-signal modulation regime, the laser current is given by [34]

$$I(t) = I_0 + I_s(t), \quad (27)$$

where I_0 is the DC value of the current injected into the active region, while $I_s(t)$ is the amplitude of the AC current component. For a small modulation, the state variables can be written as their steady-state values (N_0 , P_0 , ϕ_0) plus modulation terms ($N_s(t)$, $P_s(t)$, $(\phi_s(t))$) as [34]

$$N(t) = N_0 + N_s(t), |N_s(t)| \ll N_0 \quad (28a)$$

$$P(t) = P_0 + P_s(t), |P_s(t)| \ll P_0 \quad (28b)$$

$$\phi(t) = \phi_0 + \phi_s(t), |\phi_s(t)| \ll \phi_0 \quad (28c)$$

By substituting Eq. (27) and Eq. (28) in Eq. (11), we obtain

$$\begin{aligned} \begin{bmatrix} dN_s(t) \\ dP_s(t) \\ d\phi_s(t) \end{bmatrix} &= \begin{bmatrix} -\left(\frac{1}{\tau_{c,fe}}\right) - \left(\frac{\Gamma v_g a_0 P_0}{V}\right) & -\Gamma v_g g(1 - \Gamma \varepsilon P_0) & 0 \\ \frac{1}{V} (\Gamma v_g P_0 + 2\beta_{sp} B N_0) & \left(\frac{-R_{sp}}{P_0}\right) - \Gamma^2 \varepsilon v_g g & 0 \\ \frac{1}{2V} (\Gamma v_g a_0) & 0 & 0 \end{bmatrix} \\ &\times \begin{bmatrix} N_s(t) \\ P_s(t) \\ \phi_s(t) \end{bmatrix} + \begin{bmatrix} I_s(t)/q \\ 0 \\ 0 \end{bmatrix}. \end{aligned} \quad (29)$$

Equation (29) shows that the modulation current changes the carrier and photon populations inside the active region, which in turn affects the optical phase. However, because of intrinsic laser resonance, the modulation response is frequency dependent. Modulation of the current leads to power modulation in addition to optical frequency affects. This is seen clearly in Eqs. (11a) and (11c). The lasing frequency is shifted during modulation by an amount of [34]

$$\Delta v(t) = \frac{1}{2\pi} \left[\frac{d\phi(t)}{dt} \right]. \quad (30)$$

Performing Fourier transform to Eq. (11), the TD frequency modulation (FM) response becomes

$$\begin{aligned} \text{FM}(\omega, T) &= \frac{\alpha G_N(T)}{4\pi q} \\ &\times \left(\frac{\omega^2 + \zeta_{fe}^2(T)}{(\omega^2 - \Omega_{fe}^2(T) - \Psi_{fe}^2(T))^2 + (2\omega \Psi_{fe}(T))^2} \right)^{1/2}, \end{aligned} \quad (31)$$

where $\zeta_{fe}(T) = (R_{sp,fe}(T)/P_0) + \Gamma^2 \varepsilon(T) v_g(T) P_0$, $\Omega_{fe}(T)$ is the TD angular frequency of relaxation oscillations given as [34]

$$\begin{aligned} \Omega_{fe}(T) &= \left[\frac{1 + G_N(T) V N_0 \tau_{p,fe}(T)}{[A_{nr} + B N_{th,fe}(T) + C N_{th,fe}^2(T)]^{-1} \tau_{p,fe}(T)} \right. \\ &\times \left. \left(\frac{I}{I_{th,fe}(T)} - 1 \right) \right]^{1/2}, \end{aligned} \quad (32)$$

and $\Psi(T)$ is the TD decay rate of the relaxation oscillation defined as [34]

Link to full text articles :

<http://adsabs.harvard.edu/abs/2015OptRv.tmp...44H>

<http://link.springer.com/article/10.1007/s10043-015-0064-y>